PN Modification of Stereopure GalNAc-siRNAs Enhances Durability of Human *HSD17B13* Silencing in Transgenic Mouse Model

Wei Liu, Naoki Iwamoto, Subramanian Marappan, Khoa Luu, Snehlata Tripathi, Erin Purcell-Estabrook, Juili Dilip Shelke, Himali Shah, Anthony Lamattina, Qianli Pan, Brett Schrand, Frank Favaloro, Mugdha Bedekar, Arindom Chatterjee, Jigar Desai, Tomomi Kawamoto, Genliang Lu, Jake Metterville, Milinda Samaraweera, Priyanka Shiva Prakasha, Hailin Yang, Yuan Yin, Hui Yu, Paloma H. Giangrande, Michael Byrne, Pachamuthu Kandasamy, Chandra Vargeese

Wave Life Sciences, Cambridge, MA, USA

Summary

- We applied PS and PN backbone chemistry and stereochemistry (**Figure 1A**) to GalNAc-siRNAs with enhanced stability (**Figure 1B**).[1,2]
- We evaluated their impact on silencing for multiple liver targets: *Transthyretin* (mouse *Ttr*) and the clinically relevant liver gene *Hydroxysteroid 17-beta dehydrogenase 13* (human *HSD17B13*)[3] and explored mechanisms driving improvements in silencing.[4]
- For the antisense strand, when 2′-deoxyfluoro (2′-F) content is reduced, 5′-*Sp*Rp PS and 5′-*Rp*Sp PS modifications both work well; 3′-SpSp PS modification is favored due to interactions with PAZ domain of Ago2 and increased stability.
- The impact of PN backbone on activity depends on its position in the backbone, the chirality of the linkage, and nearby 2′-ribose modifications.
- Potency and durability benefits observed in mice with stereopure GalNAc-siRNAs are driven by improved Ago2 loading compared with reference GalNAc-siRNA formats. Improved Ago2 loading results from Ago2 interaction with chiral PN modifications in the seed region, as well as thermal instability introduced by PN modifications.
- Chimeric backbone chemistry is applicable to all oligonucleotide modalities, including silencing with RNase H and RNAi, exon skipping, and RNA editing.

Figure 1. Introduction to PN chemistry

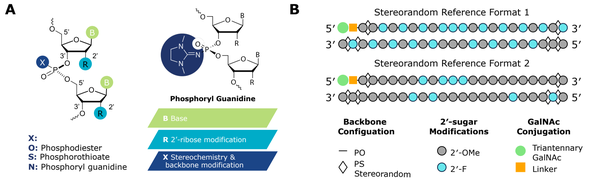

Results

Figure 2. Structure-activity assessments reveal key design features

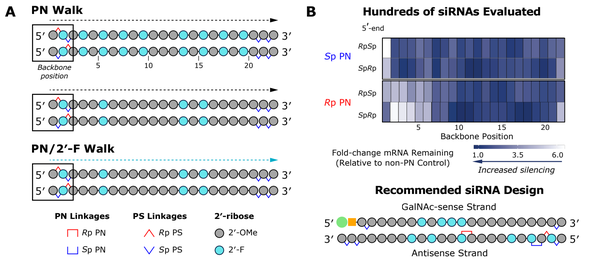

(B) Mouse primary hepatocytes were treated with GalNAc-siRNAs for 48 h. *Ttr* mRNA was quantified by RT-PCR. Expression was standardized to *Hprt* expression in the same sample and normalized to standardized *Ttr* expression for the reference compound which lacked PN modification.

- We evaluated the impact of stereopure PS and PN backbone chemistry on GalNAc-siRNA activity in primary mouse hepatocytes by "walking" the stereopure linkages through the backbone of the antisense strand for both siRNA formats. For the format with reduced 2′-F content, the activity with PN linkages was influenced by adjacent 2′-ribose modifications, so walks were repeated with PN in combination with 2′-F modification on the 3′-side of the PN linkage (**Figure 2A**).
- Activity profiles for hundreds of stereopure siRNAs were generated. An exemplary heat map from one series of siRNAs is shown (**Figure 2B**).

Figure 3. Incorporation of PN chemistry increases *Ttr* silencing by promoting Ago2 loading

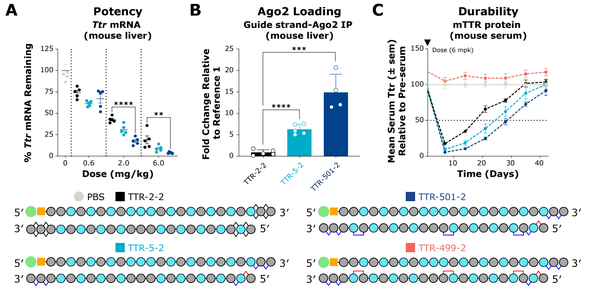

(A) C57BL/6J mice were treated with 0.6, 2, or 6 mg/kg of the indicated siRNA or PBS by SC injection on day 0. Liver Ttr mRNA levels were quantified by RT-PCR 1-week later. Stats: 2-way ANOVA with post-hoc comparison to TTR-2-2. ** P<0.01, **** P<0.0001. (B) Ago2 loading was quantified by RT PCR from livers in panel A after 1 week of treatment with 2 mg/kg siRNA. Stats: Welch's 1-way ANOVA with post-hoc comparison to TTR-2-2. *** p<0.001, **** P<0.0001. (C) Mice were treated with 6 mg/kg of the indicated siRNA or PBS by SC injection, and serum Ttr protein levels were assessed each week by ELISA through the end of the experiment.

- We compared the activity of a stereopure siRNA containing an optimal configuration of PS linkages (TTR-5-2) to one with the addition of stereopure PN linkages (TTR-501-2) to one based on stereorandom reference format 1 (TTR-2-2) in mice.
- One-week post-injection, all GalNAc-siRNAs led to dose-dependent decreases in *Ttr* mRNA in mouse liver (**Figure 3A**). The stereopure siRNAs were more potent than TTR-2-2, and TTR-501-2 had increased potency compared with both TTR-5-2 and TTR-2-2.
- We evaluated Ago2 loading 1-week post-injection. TTR-5-2 and TTR-501-2 elicited more Ago2 loading than TTR-2-2, as measured by loading of the guide strand, and TTR-501-2 showed the largest Ago2 loading advantage (**Figure 3B**).
- In a longer experiment, TTR-2-2 led to maximum decrease in serum Ttr protein levels (83%) ~1-week post-dose, with Ttr protein levels recovering until day 35 when they matched levels in mice treated with PBS. The stereopure siRNAs followed the same general pattern but with greater maximal silencing (TTR-5-2 91%; TTR-501-2 95%) that remained significantly lower than TTR-2-2 for most of the experiment ($p<0.01$, linear mixed effects model) (**Figure 3C**). We also included TTR-499-2, an siRNA with the opposite configuration of PN linkages to TTR-501-2. TTR-499-2 had silencing activity comparable to PBS (**Figure 3C**).

Figure 4. Silencing with PN chemistry impacted by adjacent 2′-ribose modifications

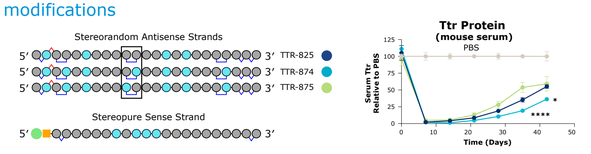

C57Bl/6J mice administered siRNAs on day 0, serum Ttr protein measured (ELISA) through day 42. Stats *P<0.01, **** P<0.0001 linear mixed-effects ANOVA with post-hoc test comparing TTR-874 to TTR-875.

- For Reference format 2, with reduced 2′-F content, the 2′-ribose modification pattern influenced silencing activity.[4]
- We generated 3 stereopure GalNAc-siRNAs with variable 2′-ribose modifications associated with a central *Sp* PN linkage.
- TTR-874, which contains a 2′-F modification on the 3′-side of the PN linkage, was the most active, increasing *Ttr* silencing observed at later time points compared with TTR-875, which has a 2′-F on the 5′-side of the PN linkage (**Figure 4**).

Figure 5. Incorporation of PN chemistry does not affect endogenous RNAi pathways in primary mouse hepatocytes

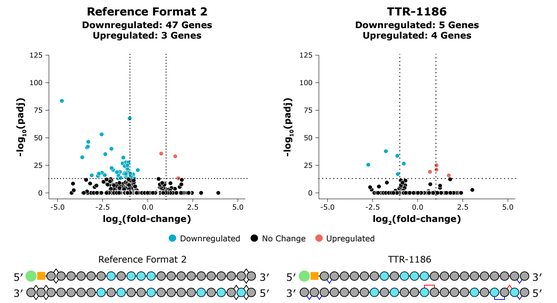

Primary mouse hepatocytes were treated with the indicated GalNAc-siRNA. Gene expression was evaluated by RNA-seq. Genes expression changes are indicated.

- We evaluated mRNA expression in mouse hepatocytes after treatment with GalNAc-siRNAs, and the PN-containing molecule had a limited impact on gene expression patterns (**Figure 5**), indicating that it does not disrupt endogenous RNAi pathways.

Figure 6. PN-modified *HSD17B13* GalNAc-siRNA shows Ago2-loading advantage and more durable silencing in mice

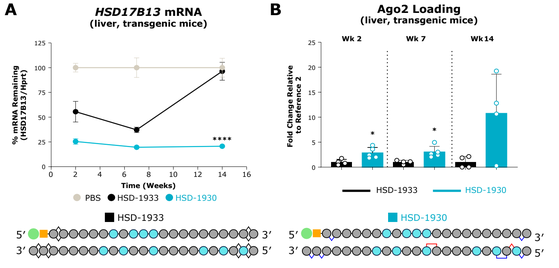

Mice expressing a human *HSD17B13* transgene were treated with 3 mg/kg of the indicated siRNA or PBS, and liver mRNA, guide strand concentration, and Ago2 loading were quantified at the indicated times post-dose. Stats: 2-way ANOVA with post-hoc comparisons to HSD-1933. * P<0.05, ****P<0.0001.

- We applied the same general GalNAc-siRNA design from *Ttr* to HSD17B13 and evaluated its activity in human *HSD17B13* transgenic mice.
- At 2-weeks post-dose, the control HSD-1933 (Reference 2 format) exhibited a mean silencing of ~45%. HSD-1930 (the PN-containing stereopure GalNAc-siRNA) led to more mean silencing (~75%). By 7-weeks post-dose, HSD-1933 reached ~60% silencing, whereas HSD-1930 reached ~80% silencing. By 12 weeks post-dose, these differences increased, with *HSD17B13* mRNA levels recovering in samples treated with HSD-1933 (mean silencing: ~5%) but remaining significantly suppressed in HSD-1930-treated samples (mean silencing: ~80%; $p<0.0001$, linear mixed effects model) (**Figure 6A**).
- Differences in silencing corresponded to an increase in Ago loading for HSD-1930 (**Figure 6B**).

Figure 7. PN backbone configurations impact Ago2 loading in the seed region

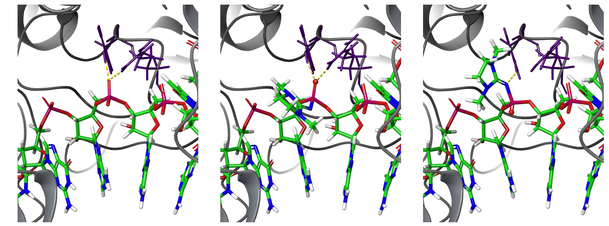

- We modeled *Sp* and *Rp* PN linkages in seed region using crystal structures of human AGO2.[5,6]
- Most interactions between AGO2 and RNA are mediated by the phosphate backbone, and we illustrate position 3 as an example. Arg792 and Tyr790 (purple) interact via hydrogen bonds (H bonds, yellow) with a non-bridging oxygen of the PO backbone (red) at position 3 (**Figure 7A**).
- With an *Sp* PN linkage, these H bonds are preserved, and the guanidine moiety is positioned away from the protein (**Figure 7B**).
- With an *Rp* PN linkage, these H bonds are disrupted, and the guanidine moiety projects into AGO2, creating steric interference (**Figure 7C**).

Table 1. PN linkages in the seed region increase thermal instability to promote Ago2 loading

Name	Format 1	Tm (°C)
Sense-1	5′ ●●●●●●●●●●●●●●●●●●●● 3′	
TTR-5	5′ ●●●●●●●●●●●●●●●●●●●● 3′	69.6
TTR-718	5′ ●●●●●●●●●●●●●●●●●●●● 3′	68.7
TTR-696	5′ ●●●●●●●●●●●●●●●●●●●● 3′	67.8
Name	**Format 2**	**Tm (°C)**
Sense-2	5′ ●●●●●●●●●●●●●●●●●●●● 3′	
TTR-1237	5′ ●●●●●●●●●●●●●●●●●●●● 3′	65.5
TTR-1165	5′ ●●●●●●●●●●●●●●●●●●●● 3′	64.7
TTR-1147	5′ ●●●●●●●●●●●●●●●●●●●● 3′	64.8

- We assessed the thermal stability (Tm) of GalNAc-siRNAs for both Reference format 1 and Reference format 2 configurations (**Table 1**). For TTR-5 (stereopure format 1 no PN linkages), the measured Tm was 69.6°C. Adding a PN linkage at position 3 (*Sp* PN: TTR-718, *Rp* PN: TTR-696) lowered Tm by ~1°C.
- For TTR-1237, (stereopure format 2 no PN linkages), the Tm decreased again by ~1°C by the addition of a PN linkage at position 3 (*Sp* PN: TTR-1165, *Rp* PN: TTR-1147), indicating that the inclusion of PN linkages increases thermal instability (**Table 1**).

References: 1. Nair et al., 2017. *Nucleic Acids Res.*, 45, 10969–10977; 2. Foster et al., 2018. *Mol. Ther.*, 26, 708–717; 3. Abul-Husn et al., 2018. *N. Engl. J. Med.*, 378, 1096–1106; 4. Liu et al., 2023. *Nuc Acids Res.*, doi: 10.1093/nar/gkad268; 5. Schirle and MacRae., 2012. *Science*, 336, 1037–1040; 6. Elkayam et al., 2012. *Cell*, 150, 100–110. **Acknowledgments:** Editorial and graphical support provided by Amy Donner (Wave Life Sciences) and Eric Smith, respectively.